



## Efficient Removal of Pb (II) from aqueous waste by manganese oxide/modified activated carbon composites

H.I. El-Ahwany<sup>1\*</sup>, W. M. Abdellah<sup>2</sup>, R. El-Sheikh<sup>1</sup>

<sup>1</sup>Chemistry Department, Faculty of Science, Zagazig University, Egypt

<sup>2</sup>Radiation Protection Department, Egypt Nuclear and Radiological Regulatory Authority, Cairo, Egypt

Received 15 Feb. 2020  
Accepted 5 Aug. 2020

The present composites (NMO/Modified AC) were prepared and utilized for the removal of Pb (II) from waste water through batch adsorption. Nano manganese oxide (NMO) was prepared by simple co-precipitation method / modified activated carbon which was treated with HNO<sub>3</sub> (4M, 6M and 8M). The synthesized samples NMO, NMO/(4M,6M,8M) AC and AC were characterized using X-Ray Diffraction (XRD), Fourier transform infrared spectroscopy (FT-IR) and Scanning Electron Microscope (SEM). Batch experiments were carried out under several conditions including pH, temperature, contact time, competing cation, and initial lead(II) ion concentration to remove lead (II) ions from liquid waste water. The results revealed that NMO, NMO / (4M, 6M, 8M) AC, and AC have a high adsorption efficiency (>99%). The adsorption results from the applied experiments fit the Langmuir isotherm, and the kinetic data follow pseudo-second-order model. In addition, the evaluation of thermodynamic parameters ( $\Delta G^\circ$ ,  $\Delta S^\circ$  and  $\Delta H^\circ$ ) from Van't Hoff equation indicated the spontaneous and exothermic nature of the adsorption.

**Keywords:** Lead/ Activated carbon/ Manganese oxide/ Co-precipitation/ Adsorption

### Introduction

Lead (Pb) ions are considered a worldwide pollutant element and are classified as hazardous heavy metal with high priority in the perspective of human and environmental risk because it is commonly detected in several industrial wastewaters [1]. Waste from metallurgy, electroplating, storage battery, paint, electronics, petroleum refining industries etc. released into water bodies is a major source of Pb (II) pollution [2]. It is necessary to remove lead ions from wastewater to bring it down to an acceptable level for better life. Heavy metal ions such as lead could be eliminated by several traditional techniques, including chemical precipitation, electrochemical treatment techniques, reverse osmosis, membrane

filtration, coagulation, ion exchange, adsorption, irradiation and extraction [3, 4, 5, 6, 7, 8, 9, 10, 11, 12]. Adsorption is the most commonly used process it is a fairly simple and convenient unit operation and the cost for its application is relatively low compared to other treatment processes. The use of adsorption contacting system for industrial and municipal wastewater treatment has become prevalent during recent years [13]. Adsorption is frequently utilized toward the end of a treatment sequence for pollution control due to the high level of purification that can be accomplished. Manganese oxide, one of the most widely studied transition metal oxides, has attracted more and more attention due to its wide

application in many fields, such as wastewater treatment, catalysis, sensors, supercapacitors, lithium ion batteries [14, 15, 16, 17, 18, 19, 20].

Nano manganese oxide (NMO) has a particular advantages of a high storage capacity, low cost, lower thermodynamic equilibrium voltage versus  $\text{Li/Li}^+$ , and environmental friendliness [15,21].

Activated carbon is a black solid substance looking like granular or powder charcoal and is carbonaceous material that has a highly created porosity, internal surface area of more than  $400\text{m}^2\text{g}^{-1}$  and relatively high mechanical strength [22]. It is broadly utilized as adsorbents in wastewater and gas treatments just as in catalysis, to improve the adsorption capacity for heavy metals, modification of activated carbon has been proposed [23]. It has been demonstrated that heavy metals adsorption by activated carbon extraordinarily depends upon surface acidity and special surface functionality, where the removal mechanisms may include electrostatic interaction, coordination and ion exchange to functional groups [24,25]. A typical method to improve lead adsorption is through substance oxidation, which is able to introduce a variety of acidic surface functional groups on the surface of activated carbon [26]. A variety of oxidizing agents such as  $\text{HNO}_3$ ,  $\text{KMnO}_4$ ,  $\text{H}_2\text{O}_2$ ,  $(\text{NH}_4)_2\text{S}_2\text{O}_8$  and  $\text{NaOCl}$  have been widely utilized [27,28]. Nitric acid is the most frequently used one, as its oxidizing specifications can be controlled by concentration and temperature. During oxidation, the surface characteristics of activated carbon are changed due to the introduction of new functional groups such as carboxylic, phenolics, lactones and carbonyl, which can eventually extend the adsorption capacity towards lead (II) [29].

### Aim of the work

The main purpose of the present work is to explore the possibilities of using low cost composites NMO, NMO/(4M,6M,8M) AC and AC for the adsorption of lead (II) from wastewater resulting from different industrial fields such as metallurgy, electroplating, storage battery ,paint, electronics and petroleum refining industry. The influence of several operating parameters for the removal of lead(II) Such as pH, contact time, temperature, initial concentration, competing cation, etc. were studied in a batch technique. The adsorption isotherms Langmuir and Freundlich as well as

kinetic isotherm pseudo-first order and pseudo-second order models are investigated.

## 2. Materials and methods

### 2.1. Chemicals and reagents

All chemicals were of analytical grade, purchased and used as received without further purification. Manganese chloride  $\text{MnCl}_2 \cdot 4\text{H}_2\text{O}$ ; Merk, potassium permanganate  $\text{KMnO}_4$ ; Sigma-Aldrich, activated carbon (AC) commercial one, lead nitrate  $\text{Pb}(\text{NO}_3)_2$ ,  $\text{HNO}_3$ ,  $\text{HCl}$  and  $\text{NaOH}$  were used throughout the investigations. Bi-distilled water was used through all experiments.

A standard lead solution (II) was used (1000 ppm). Thus standard solution (1000 ppm) was diluted to obtain different desired concentration ranging from 20 to 200 ppm as demonstration to the industrial liquid waste.

Preparation and characterization of composites under this investigation were reported and published by Abdellah et al. [30].

### 2.2. Adsorption experiments

The batch adsorption experiments were performed by contacting 0.05g of the selected adsorbent with 10 ml of  $\text{Pb}(\text{II})$  ion solutions into polypropylene centrifuge tube. The experiments were performed in a shaker with a constant agitation speed (200 rpm) for 2 hours. The suspension was passed through  $0.45\ \mu\text{m}$  cellulose nitrate membrane syringe filter diameter 25mm. The effect of initial pH, contact time, initial concentration of adsorbate  $\text{Pb}(\text{II})$ , competing cation and temperature were investigated. The pH of solutions was adjusted at the desired value by adding 0.1M  $\text{NaOH}$  or  $\text{HCl}$ , the remaining concentration of lead(II) in each sample was determined by the use of simultaneous inductively coupled plasma emission spectrometer (720 ICP-OES, Agilent Technologies) at the Egyptian Mineral Resources General Authority, Cairo.

The adsorption capacity of  $\text{Pb}(\text{II})$   $q_t$  (mg/g) was calculated using equation (1).

$$q_t = \frac{(C_o - C_t) V}{m} \quad (1)$$

Where  $C_o$  (mg/L) is the initial concentration of  $\text{Pb}(\text{II})$   $C_t$  (mg/L) is the concentration of  $\text{Pb}(\text{II})$  after filtration at time t, V is the volume of  $\text{Pb}$  in (L) (II) ions solution, and m(g) the mass of sorbent. The percent uptake or the removal efficiency (R%) was calculated from the equation (2).

$$R\% = \frac{(C_0 - C_t)}{C_0} \times 100 \quad (2)$$

At equilibrium the quantity adsorbed  $q_e$  (mg/g) from equation (3).

$$q_e = \frac{(C_0 - C_e) V}{m} \quad (3)$$

Where,  $C_e$  (mg /g) is the Pb(II) concentration at equilibrium,  $C_0$  (mg/L) is the initial concentration of Pb(II) ions,  $V$  (L) is the volume of Pb(II) ions solution, and  $m$ (g) the mass of adsorbent [31].

### 3. Results and discussion

#### 3.1. Adsorption experiments

##### Effect of solution pH

The pH of the solution obviously influenced the removal efficiency of the Pb (II) ions in aqueous solutions which controls the surface charge of the adsorbent and has a significant effect on the behavior of Pb (II) ions. We used  $\text{HNO}_3$  and  $\text{NaOH}$  were used to adjust the pH. The pH effect was studied below six to avoid the precipitation of lead (II) [32, 33] hence, the pH values were varied between  $2 \pm 0.1$  and  $6 \pm 0.1$ , keeping the other parameters constant adsorbent weight (0.05g), initial Pb (II) concentration (20 ppm), contact time (120 min), agitation speed (200 rpm) and at room temperature.

**Figure (1)** shows no effect of the percent uptake in case of the adsorbents NMO and NMO / (4M,6M,8M) AC by changing pH from  $2 \pm 0.1$  to  $6 \pm 0.1$ . This may be an important advantage of NMO and NMO/(4M,6M,8M) AC to be used over a wide range of pH, especially when compared with the obtained results of nano metal oxides and composites. In the case of using AC as adsorbent, the maximum percent uptake of Pb (II) was about 99.3% at pH 6. The increase in Pb (II) removal with increase in pH values can be explained on the basis of a decrease in the competition between proton and lead cations for the same functional groups and by the decrease in the positive charge of the AC which results in a lower electrostatic repulsion between the lead cations and the surface of AC [34].

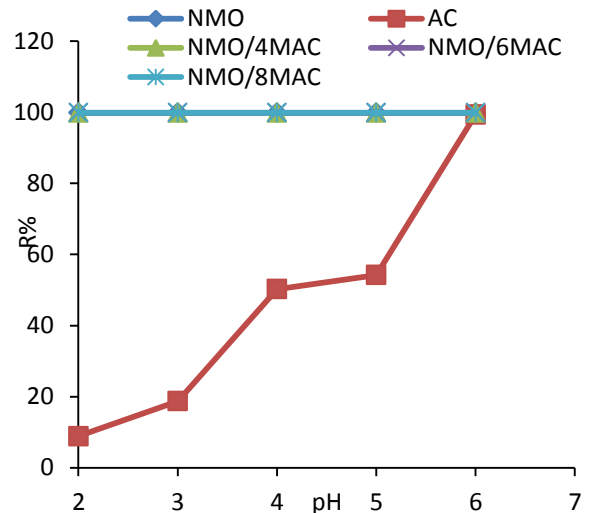


**Figure 1.** Effect of pH on Pb(II) removal percent for samples NMO, NMO/4M AC, NMO/6M AC, NMO/8M AC and AC

##### Effect of contact time

**Figure 2(A, B, C, D, E)** Illustrates that Pb(II) removal was increased with increasing the time before equilibrium was reached. Keeping the other parameters constant, the adsorbent weight (0.05g), initial Pb(II) concentration (20 ppm), pH ( $5 \pm 0.1$ ), agitation speed (200) rpm and at room temperature. It was revealed that the adsorption capacity of NMO, NMO / (4M,6M,8M) AC and AC adsorbents for the removal of Pb(II) ion increased rapidly in the first 15 min, it was about 99.5%, 99.6%, 99.5% and 99.5% respectively for NMO, NMO / (4M,6M,8M) AC and 58.7% for AC after a contact time of 3 h. Hence, the optimum contact time for NMO, NMO / (4M,6M,8M) AC was chosen to be 1 h and for AC is 2 h because the adsorption process reached the equilibrium at that time and remained constant.

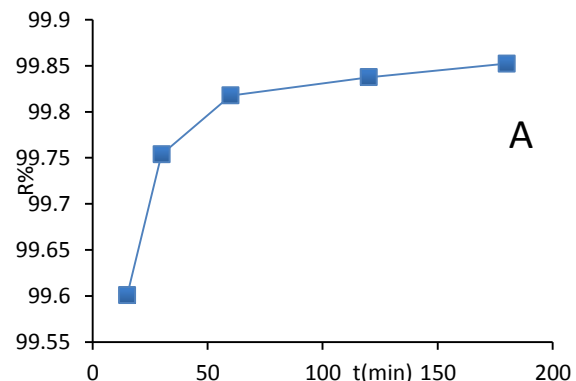


**Figure 2(A).** Effect of contact time on Pb(II) removal percent by sample NMO/4M AC

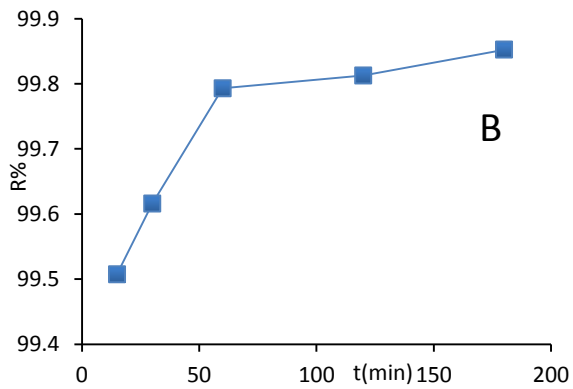


Figure 2(B). Effect of contact time on Pb(II) removal percent by sample NMO/6M AC

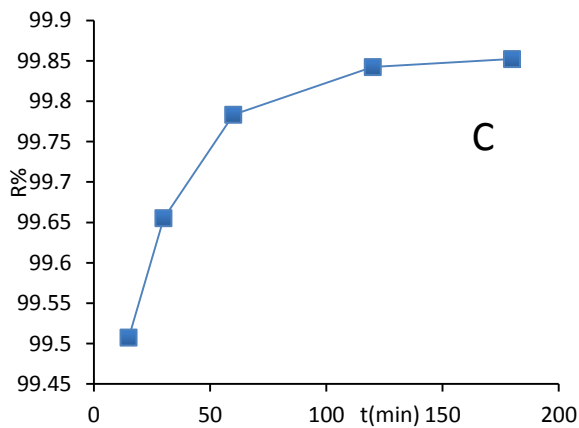


Figure 2(C). Effect of contact time on Pb(II) removal percent by sample NMO/8M AC

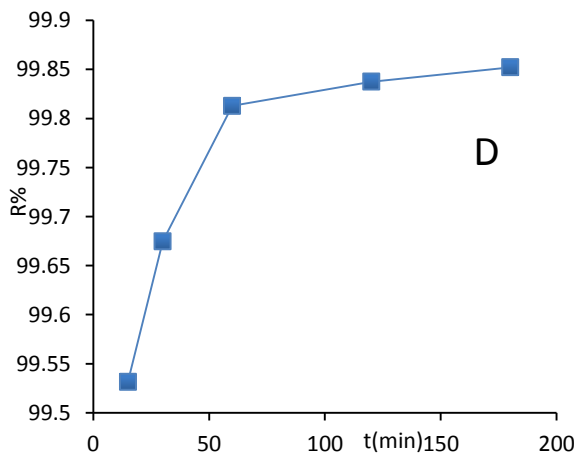


Figure 2(D). Effect of contact time on Pb(II) removal percent by sample NMO

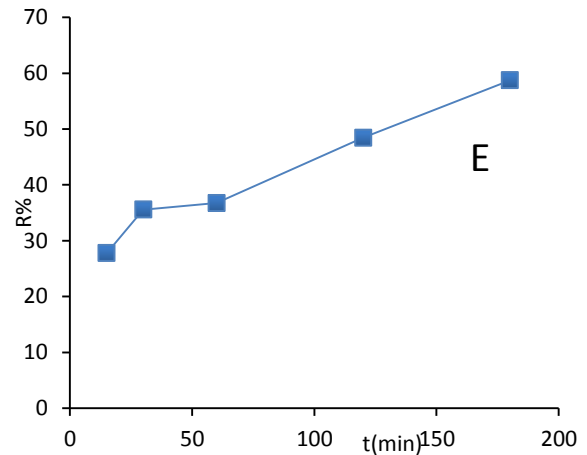


Figure 2(E). Effect of contact time on Pb(II) removal percent by sample AC

#### Effect of temperature

The effect of temperature on the adsorption of Pb(II) ions was studied from 298 to 323 K. The operating conditions used were initial lead concentration 20 ppm, adsorbent weight 0.05 g, pH ( $6.0 \pm 0.1$ ), agitation speed (200 rpm), and contact time for NMO, NMO / (4M,6M,8M) AC (1h) and (2h) for AC. The results are presented in **Figure 3(A, B, C, D, E)**. It can be observed that the percentage of lead adsorption decrease gradually with increasing temperature indicating that the process is exothermic in nature. Further, the adsorption of lead (II) is favored at low temperatures [35].

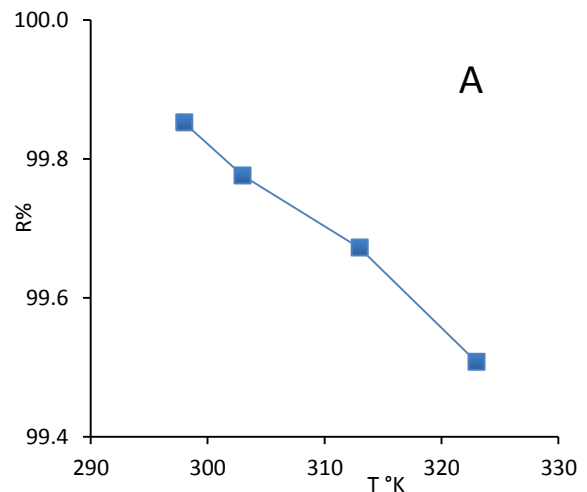


Figure 3(A). Effect of temperature on Pb(II) removal percent by sample NMO/4M AC

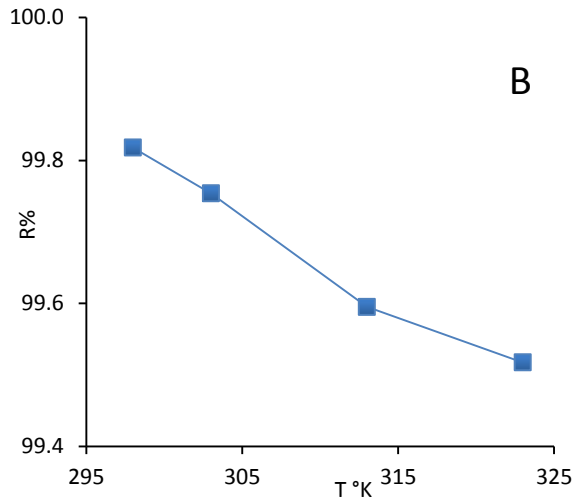


Figure 3(B). Effect of temperature on Pb(II) removal percent by sample NMO/6M AC

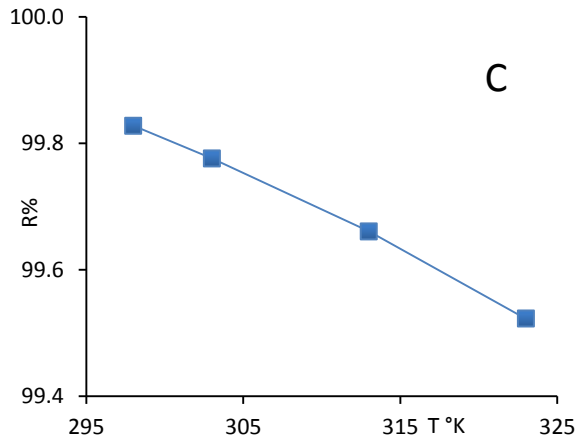


Figure 3(C). Effect of temperature on Pb(II) removal percent by sample NMO/8M AC

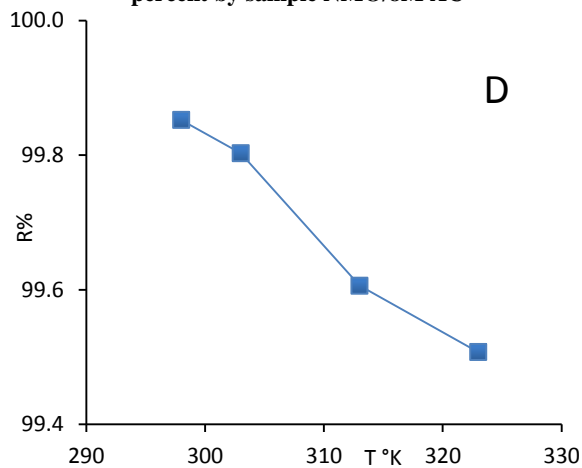


Figure 3(D). Effect of temperature on Pb(II) removal percent by sample NMO

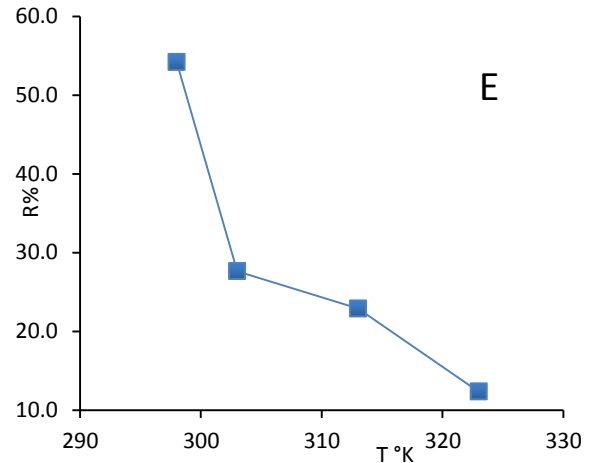


Figure 3(E). Effect of temperature on Pb(II) removal percent by sample AC

#### Effect of competing cations

The effect of competing cations on the adsorption of Pb(II) on samples NMO, NMO/4M AC, NMO/6M AC, NMO/8M AC and AC was studied using KCl salt at a variety of concentrations of KCl from 5 to 100 ppm. Keeping the other operational parameters constant, adsorbent weight (0.05g), initial Pb(II) concentration (20 ppm), pH ( $6 \pm 0.1$ ), agitation speed (200 rpm), at room temperature and contact time (1h) for NMO, NMO / (4M,6M,8M) AC and (2h) for AC. **Figure 4(A, B, C, D, E)** shows that the percentage uptake small decreases slightly as  $[K^+]$  concentration increase slightly under this investigation. These findings confirmed that  $K^+$  compete and reduce the sorption of Pb (II) ions on the five adsorbents.

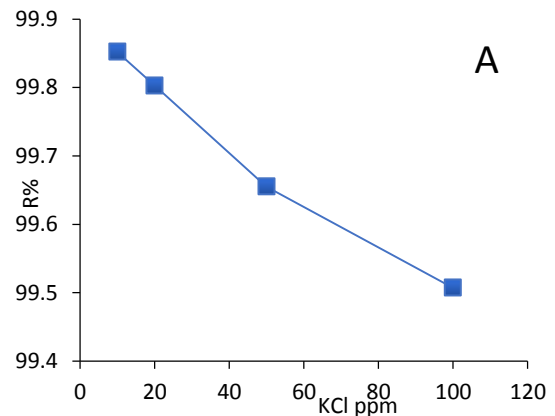


Figure 4(A). Effect of competing cations on Pb(II) removal percent by sample NMO/4M AC

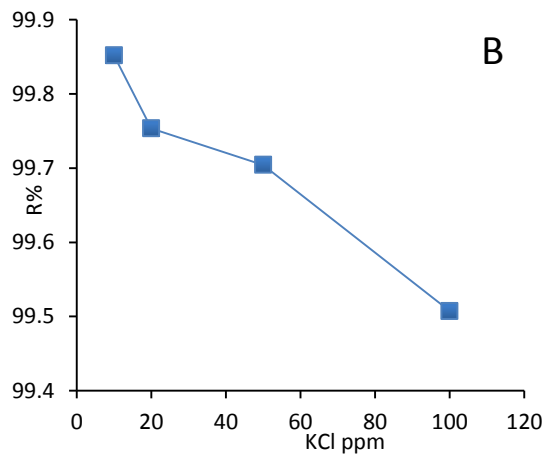


Figure 4(B). Effect of competing cations on Pb(II) removal percent by sample NMO/6M AC

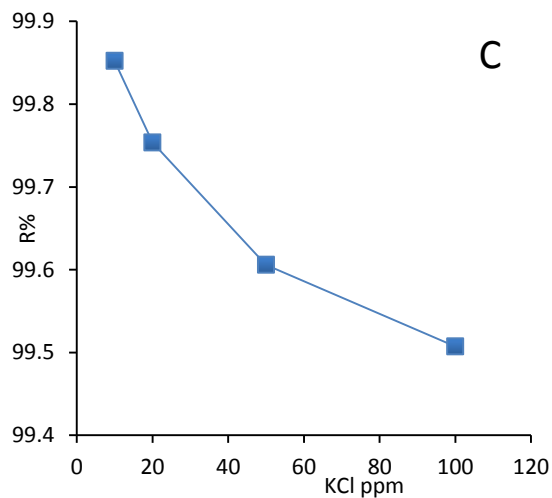


Figure 4(C). Effect of competing cations on Pb(II) removal percent by sample NMO/8M AC

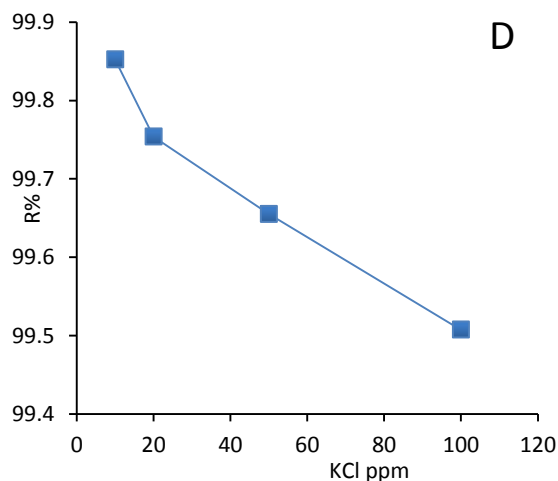


Figure 4(D). Effect of competing cations on Pb(II) removal percent by sample NMO

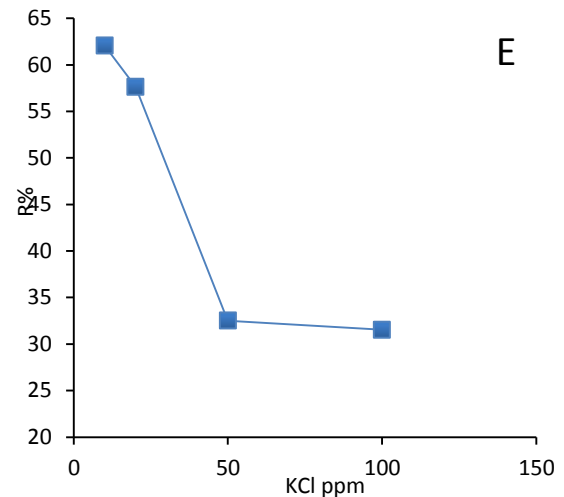


Figure 4(E). Effect of competing cations on Pb(II) removal percent by sample AC

#### *Effect of initial concentration of Pb(II)*

The effect of initial Pb(II) concentration on the adsorption rate was studied in the range 20-200 ppm. Keeping the other parameters constant, (adsorbent weight (0.05g), pH ( $6\pm 0.1$ ), agitation speed (200 rpm), at room temperature, and contact time (1h) for NMO, NMO / (4M,6M,8M) AC and (2h) for AC). The results presented in **Figure 5(A, B, C, D)** shows that the adsorption capacity increased with increasing the initial concentration of lead (II) ions. The increase of the amount of adsorption was according to the increase in the electrostatic interaction between the lead (II) ions and the adsorbent active sites due to the fact that more adsorption sites were being covered as the lead (II) ions concentration increased and this agrees with the findings of other investigators [35], but in the case of **Figure 5(E)**, there is a significant decrease due to lower active sites present in the (AC).

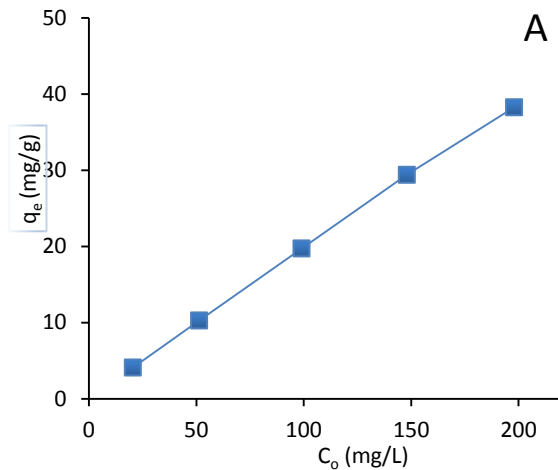


Figure 5(A). Effect of initial conc. of Pb(II) ions on the adsorption capacity by sample NMO/4M AC

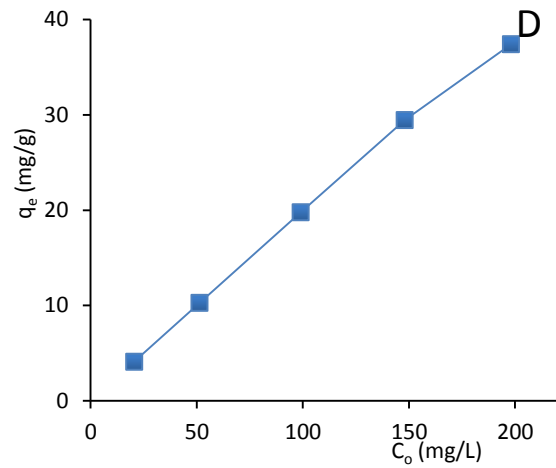


Figure 5(D). Effect of initial conc. of Pb(II) ions on the adsorption capacity by sample NMO

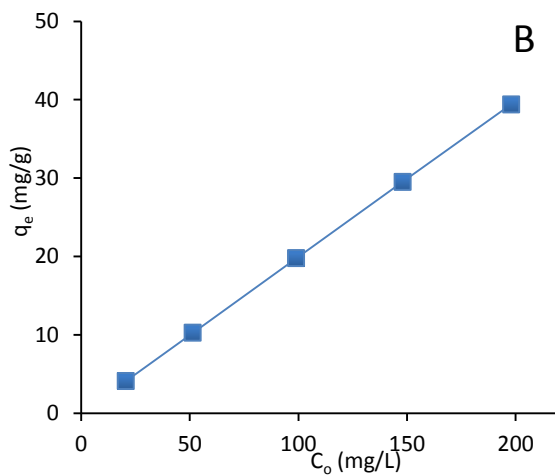


Figure 5(B). Effect of initial conc. of Pb(II) ions on the adsorption capacity by sample NMO/6M AC

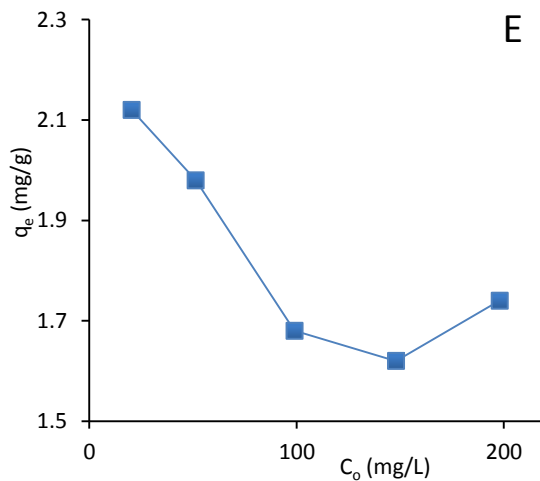


Figure 5(E). Effect of initial conc. of Pb(II) ions on the adsorption capacity by sample AC

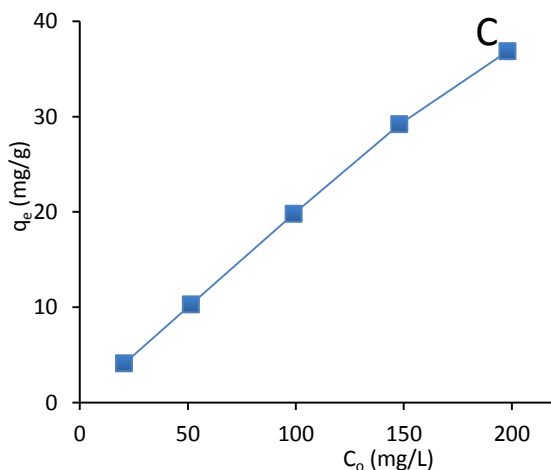


Figure 5(C). Effect of initial conc. of Pb(II) ions on the adsorption capacity by sample NMO/8M AC

### 3. 2. Adsorption Isotherm

Adsorption is the process in which lead (II) ions are adsorbed on NMO, NMO / (4M,6M,8M) AC, and AC surface, and the equilibrium is established when the concentrations of lead (II) ions adsorbed and in water become constant. At equilibrium, the relationship between the amounts of lead (II) ions adsorbed and in water is called an adsorption isotherm [36]. From these isotherms, several adsorption parameters could be calculated.

#### Langmuir isotherm model

This empirical model assumes monolayer adsorption onto a surface containing a finite (fixed) number of adsorption sites of uniform strategies of adsorption with no transmigration of adsorbate in the plane of surface [37]. The linear Langmuir model is given by following equation (5):

$$\frac{C_e}{q_e} = \frac{1}{(q_m \cdot K_L)} + \frac{C_e}{q_m} \quad (5)$$

where  $q_e$  (mg/g) is the amount of adsorbate adsorbed per unit mass of adsorbent,  $C_e$  (mg/L) is the equilibrium concentration of the adsorbent,  $K_L$  and  $q_m$  are Langmuir constants related to adsorption capacity and rate of adsorption, respectively. A plot of  $C_e/q_e$  versus  $C_e$  would result in a straight line as shown in **Figure 6(A, B, C, D, E)**. From the slope and intercept, the maximum adsorption capacity  $q_m$  and bond energy of adsorbates can be calculated [38,39]. The essential characteristics of Langmuir isotherm can be expressed by a dimensionless constant called the separation factor or equilibrium parameter,  $R_L$ , defined by Weber and Chakkravorti [40]:

$$R_L = \frac{1}{1 + K_L C_o} \quad (6)$$

The parameter  $R_L$  indicates the shape of isotherm as given in **Table (1)** which shows that all  $R_L$  values were between 0 and 1, indicating the adsorption of lead (II) on NMO, NMO / (4M,6M,8M) AC, and AC was favorable or irreversible processes.

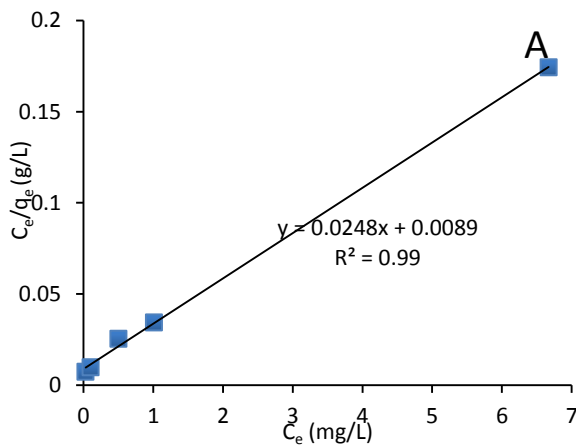


Figure 6(A). Langmuir isotherm for adsorption of Pb(II) ions on sample NMO/4M AC

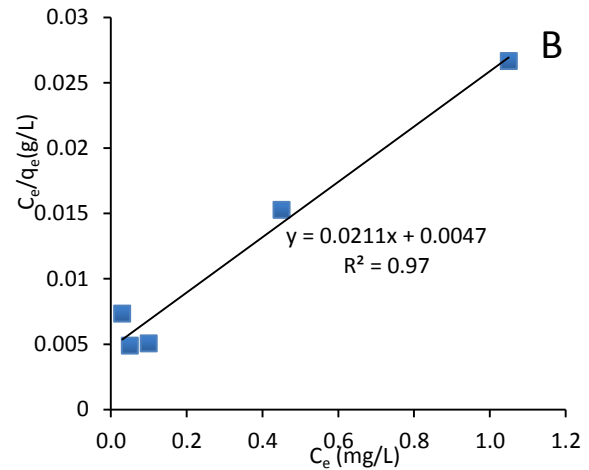


Figure 6(B). Langmuir isotherm for adsorption of Pb(II) ions on sample NMO/6M AC

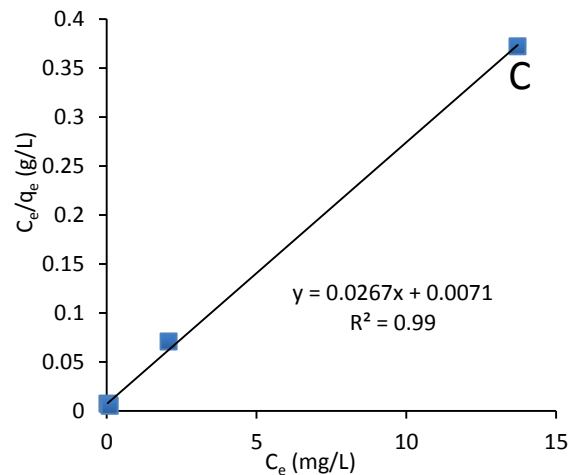


Figure 6(C). Langmuir isotherm for adsorption of Pb(II) ions on sample NMO/8M AC

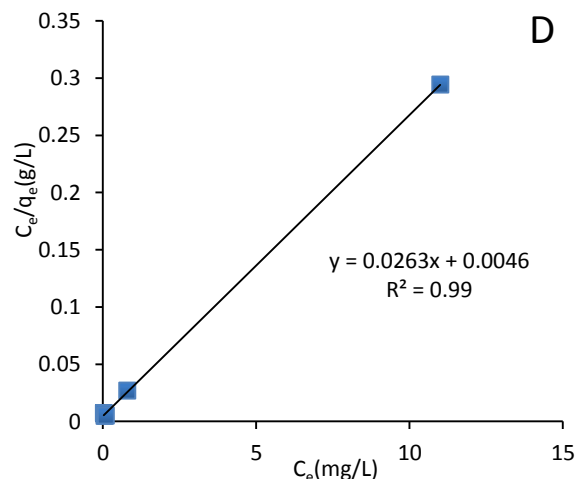


Figure 6(D). Langmuir isotherm for adsorption of Pb(II) ions on sample NMO

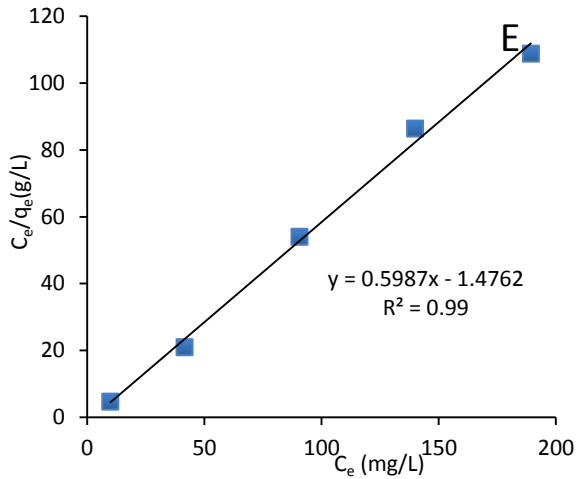


Figure 6(E). Langmuir isotherm for adsorption of Pb(II) ions on sample AC

*Freundlich isotherm model*

This empirical model assumes that the stronger binding sites are occupied first and that the binding strength decreases with the increasing degree of site occupation. This empirical equation is based on sorption on a heterogeneous surface (multilayer adsorption) or surfaces supporting sites of varied affinities [37]. The liner form of Freundlich model can be expressed by equation (7) [41]:

$$\ln q_e = \ln k_F + \left(\frac{1}{n}\right) \ln C_e \quad (7)$$

Where:  $K_F$  is the Freundlich constant (mg/g) which represents the relative adsorption capacity of the adsorbent.  $(1/n)$  is the heterogeneity factor and measure the adsorption intensity or the surface heterogeneity of the sorbent. The plot of  $\ln q_e$  versus  $\ln C_e$  gave a straight line with a slope of  $1/n$  and intercept of  $\ln K_F$ , and the value of  $1/n$  is less than 1 which indicate a favorable adsorption [42], as illustrated in Figure 7(A, B, C, D, E). and Table (1).

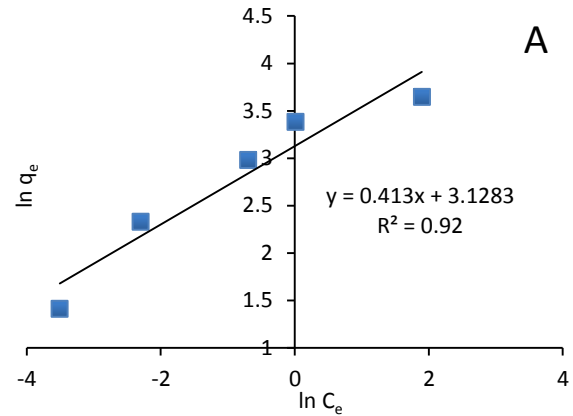


Figure 7(A). Freundlich isotherm for adsorption of Pb(II) ions on sample NMO/4M AC

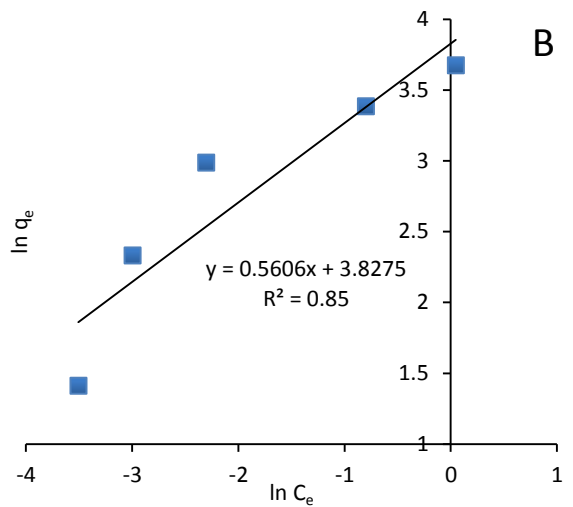


Figure 7(B). Freundlich isotherm for adsorption of Pb(II) ions on sample NMO/6M AC

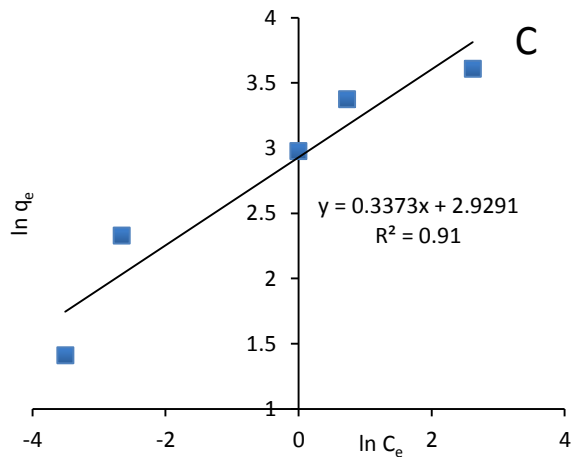


Figure 7(C). Freundlich isotherm for adsorption of Pb(II) ions on sample NMO/8M AC

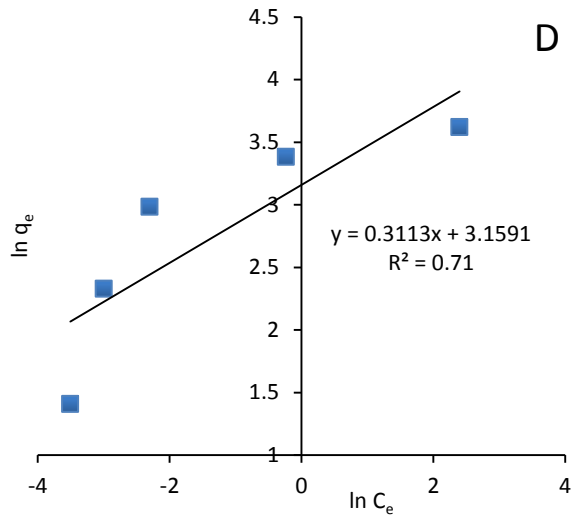


Figure 7(D). Freundlich isotherm for adsorption of Pb(II) ions on sample NMO

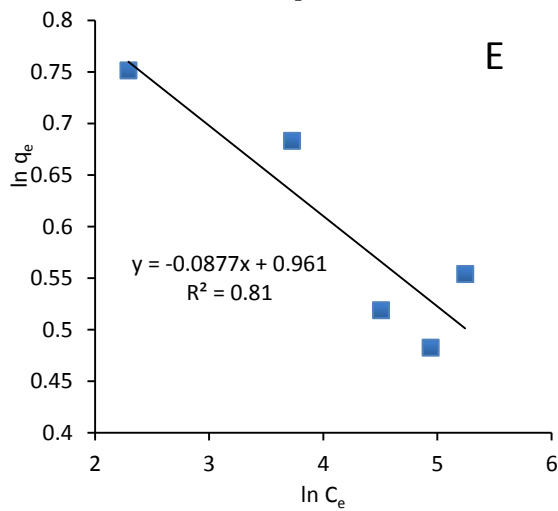


Figure 7(E). Freundlich isotherm for adsorption of Pb(II) ions on sample AC

According to the results presented in **Table (1)**, the calculated coefficients of correlation ( $R^2$ ) for both adsorbents were closer to unity, indicating a good agreement between experimental and predicted data using Langmuir model. Therefore, this model may be the more appropriate than the Freundlich model and this agrees with the findings of Goel et al. [41].

3.3 Kinetics adsorption models

The kinetic parameters of adsorption system describe the rate limiting step(s) of lead (II) ions uptake on NMO, NMO / (4M,6M,8M) AC, and AC and it controls the equilibrium time [43]. In order to predict the adsorption kinetic model for adsorption of lead (II) ions from its liquid waste onto NMO, NMO / (4M,6M,8M) AC, and AC the kinetics models: pseudo first order and pseudo second order models were applied to the experimental data. the best fit model was selected based on the linear regression correlation coefficient ( $R^2$ ), which is a measure of how the predicted values from a forecast model match with the experimental data.

Pseudo-first order model

The pseudo-first order model is the most broadly utilized to predict sorption kinetics. It expects that the rate of change of the solute uptake with time is directly proportional to the amount of solid uptake with time and the difference in the saturation concentration, for example the rate of occupation sites is directly proportional to the number of unoccupied sites [44].The model is given by Lagergren Equation or the pseudo-first order equation (8).

$$\log(q_e - q_t) = \log q_e - \frac{(k_1 t)}{2.303} \tag{8}$$

Table 1. Langmuir and Freundlich constants with R2 values obtained for removal of lead (II) ions on samples NMO/4M AC, NMO/6M AC, NMO/8M AC, NMO, and AC

Adsorbent	Langmuir				Freundlich	
	$K_L$	$q_m$	$R_L$	$R^2$	$K_F$	$1/n$
NMO/4 M AC	2.786	40.320	0.002	0.99	22.835	0.413
NMO/6 M AC	4.489	47.393	0.001	0.97	45.947	0.560
NMO/8 M AC	3.760	37.453	0.001	0.99	18.710	0.337
NMO	5.717	38.022	0.001	0.99	23.549	0.311
AC	0.405	1.670	0.012	0.99	2.614	-0.087

Where  $q_e$  and  $q_t$  denote the amounts of adsorbed lead (II) ions (mg/g) at equilibrium and at time  $t$  (min), respectively and  $k_1(\text{min}^{-1})$  is the rate constant of pseudo-first-order adsorption ( $\text{min}^{-1}$ ). A plot of  $\log(q_e - q_t)$  versus  $t$  is presented in **Figure 8(A, B, C, D, E)**, which gives a straight line to confirm the applicability of pseudo-first order kinetic model.  $\log q_e$  and  $K_1$  should be equal to intercept and slope, respectively.

Pseudo-second order model

The adsorption kinetics may also be described by a pseudo-second order model. The model assumes

that the rate of occupation of adsorption sites is proportional to the square of the number of unoccupied sites, where the rate limiting step may be the exchange of electrons between lead (II) ions and sorbent or chemical sorption involving valence forces through sharing. The pseudo-second order rate expression is used to describe chemisorption between the adsorbate and the adsorbent [45]. The linearized-integral form of the model represented in equation (9).

$$t/q_t = 1/(k_2 q_e^2) + (1/q_e)t \quad (9)$$

where  $k_2$  ( $\text{g mg}^{-1} \text{min}^{-1}$ ) is the rate constant of the pseudo-second order of adsorption. A plot of  $t/q_t$  versus  $t$  should give a straight line.  $1/q_t$  equal to the intercept and  $1/K_2 q_e^2$  the slope, which illustrated in **Figure 9(A, B, C, D, E) and Table (2)**.

The value of the correlation coefficient ( $R^2$ ) was calculated from these plots of pseudo-first order and pseudo-second order models. The linearity of these plots confirms the applicability of the two models. However,  $R^2$  in pseudo-second order model, indicating a chemisorption mechanism, fits better experimental data than the pseudo-first order model for all adsorbents. Moreover, the value of the calculated adsorption capacity  $q_e(\text{Cal})$  according to the pseudo-second order model matches with the experimentally obtained  $q_e(\text{exp})$  on comparing to the calculated from the pseudo-first order model. It could be stated that the adsorption of lead (II) ions onto NMO, NMO / (4M, 6M, 8M) AC, and AC may be obeying the pseudo-second order kinetic model [46].

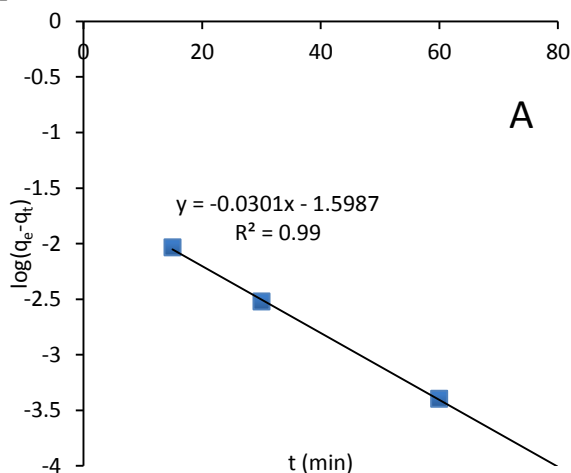


**Figure 8(A).** pseudo-first order plots for adsorption of Pb(II) ions on sample NMO/4M AC

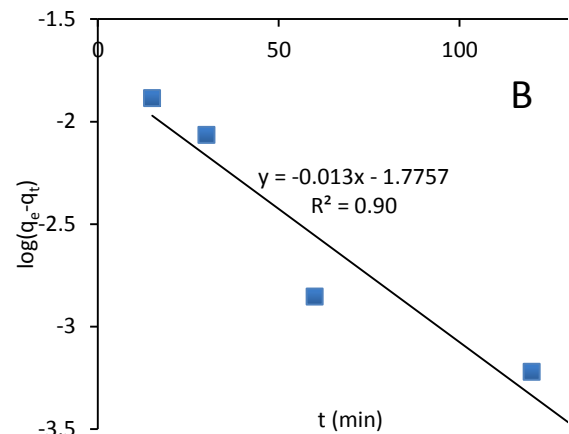


**Figure 8(B).** pseudo-first order plots for adsorption of Pb(II) ions on sample NMO/6M AC.

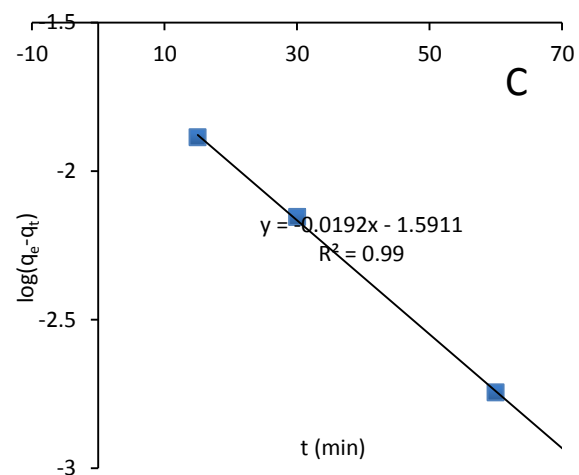


**Figure 8(C).** pseudo-first order plots for adsorption of Pb(II) ions on sample NMO/8M AC

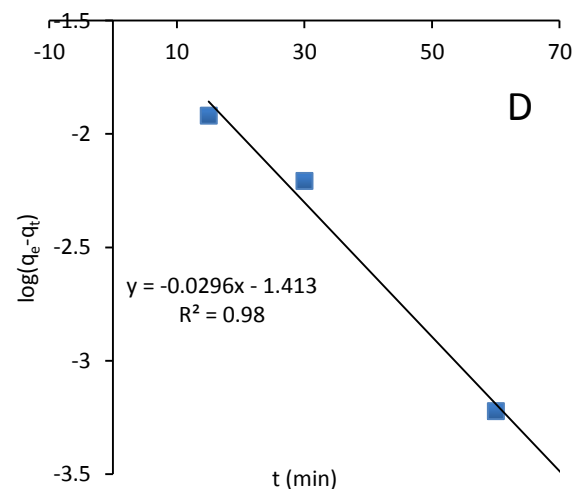


**Figure 8(D).** pseudo-first order plots for adsorption of Pb(II) ions on sample NMO

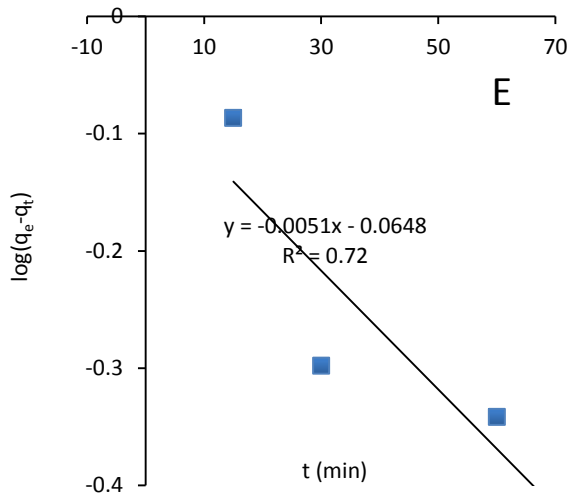


Figure 8(E). pseudo-first order plots for adsorption of Pb(II) ions on sample AC

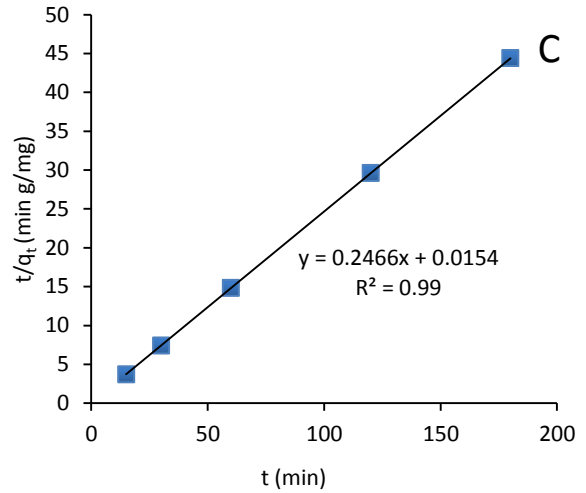


Figure 9(C). pseudo-second order plots for adsorption of Pb(II) ions on sample NMO/8M AC

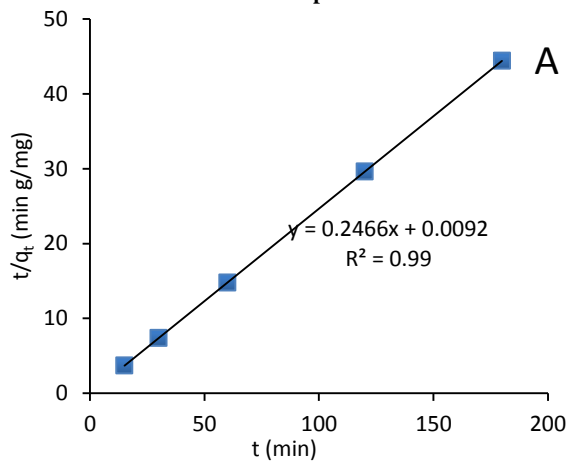


Figure 9(A). pseudo-second order plots for adsorption of Pb(II) ions on sample NMO/4M AC

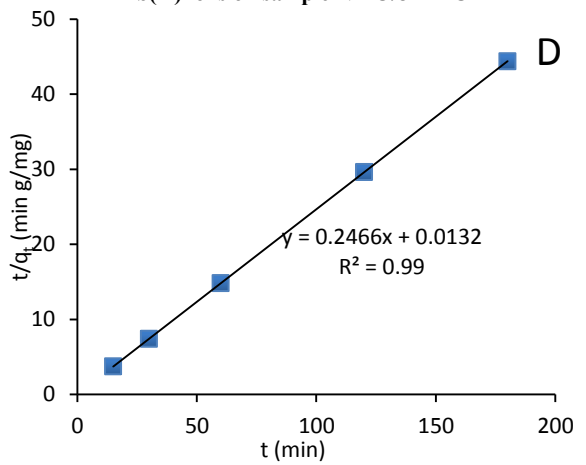


Figure 9(D). pseudo-second order plots for adsorption of Pb(II) ions on sample NMO

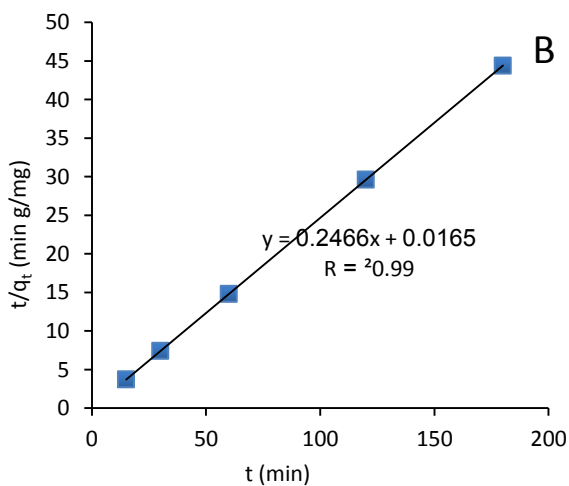


Figure 9(B). pseudo-second order plots for adsorption of Pb(II) ions on sample NMO/6M AC

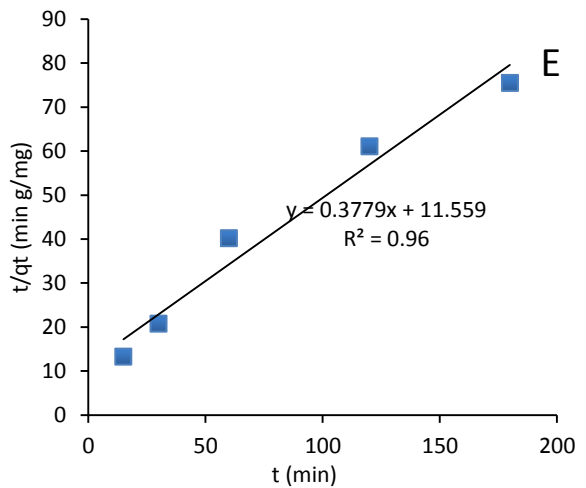


Figure 9(E). pseudo-second order plots for adsorption of Pb(II) ions on sample AC

**Table 2. Pseudo-first- second orders with R2 values obtained for removal lead (II) ions on samples NMO/4M AC, NMO/6M AC, NMO/8M AC, NMO, and AC**

Adsorbent	pseudo-first order				pseudo-second order			
	K <sub>1</sub>	q <sub>e</sub> (cal)	q <sub>e</sub> (ex)	R <sup>2</sup>	K <sub>2</sub>	q <sub>e</sub> (cal)	q <sub>e</sub> (ex)	R <sup>2</sup>
NMO/4M AC	0.069	4.053	0.025	0.99	6.610	4.053	4.055	0.99
NMO/6M AC	0.030	4.053	0.016	0.90	3.685	4.053	4.055	0.99
NMO/8M AC	0.044	4.053	0.025	0.99	3.948	4.053	4.055	0.99
NMO	0.068	4.053	0.038	0.98	4.606	4.053	4.055	0.99
AC	0.001	1.947	0.861	0.72	0.012	1.947	2.646	0.96

**Table 3.  $\Delta H^\circ$ ,  $\Delta G^\circ$  and  $\Delta S^\circ$  obtained for removal lead (II) ions on samples NMO/4M AC, NMO/6M AC, NMO/8M AC, NMO, and AC**

Adsorbent	$\Delta H^\circ$ (kJ/mol)	$\Delta S^\circ$ (J/mol K)	$\Delta G^\circ$ (kJ/mol)			
			298K	303K	313K	323K
NMO/4M AC	-36.869	-70	-15.956	-15.605	-14.903	-14.202
NMO/6M AC	-31.643	-54	-15.464	-15.193	-14.650	-14.107
NMO/8M AC	-32.404	-56	-15.701	-15.420	-14.860	-14.299
NMO	-40.186	-81	-16.040	-15.635	-14.825	-14.015
AC	-17.561	-53	-1.549	-1.280	-0.743	-0.206

### 3.4 Adsorption thermodynamics

The thermodynamic parameters such as enthalpy ( $\Delta H^\circ$ ), entropy ( $\Delta S^\circ$ ) and free energy ( $\Delta G^\circ$ ) can be evaluated from the following equations (11, 12 and 13) [47,48,49]:

$$K_d = \frac{C_{Ae}}{C_e} \quad (11)$$

$$\ln K_d = \frac{\Delta S^\circ}{R} - \frac{\Delta H^\circ}{RT} \quad (12)$$

$$\Delta G^\circ = \Delta H^\circ - T\Delta S^\circ \quad (13)$$

Where  $K_d$  is the equilibrium constant,  $C_{Ae}$  (mg/L) is the amount adsorbed on solid at equilibrium,  $C_e$  (mg/L) is the equilibrium concentration,  $R$  (8.314 J/mol K) is the universal gas constant, and  $T$  (K) is the absolute solution temperature. Plotting  $\ln K_d$  versus  $1/T$  from Van't Hoff equation (12), the values of  $\Delta S^\circ$  (J/mol K) and  $\Delta H^\circ$  (kJ/mol) were calculated from **Figure 10(A, B, C, D, E)** and presented in **Table (3)** and  $\Delta G^\circ$  (kJ/mol) can be calculated from equation (13). The negative value of ( $\Delta H^\circ$ ) indicates the exothermic nature of adsorption process for  $Pb^{+2}$  ions on NMO, NMO / (4M,6M,8M) AC, and AC. The negative value of ( $\Delta S^\circ$ ) corresponds to a decrease in the degree of freedom of the adsorbed species and suggests the probability of favorable sorption, and the negative value of  $\Delta G^\circ$  confirmed the feasibility and spontaneity of the adsorption of  $Pb^{+2}$  ions on NMO, NMO / (4M,6M,8M) AC, and AC.

### Conclusion

NMO was synthesized by a simple co-precipitation method from manganese chloride and potassium permanganate, NMO / (4M,6M,8M) AC composites were found to be an excellent adsorbent for the Pb (II) ions removal from wastewater with a removal percentage of (>99%) at an equilibrium time of 60 min for NMO, NMO / (4M,6M,8M) AC. The adsorption isotherm showed a good agreement with the Langmuir isotherm model with good correlation ( $R^2$ ). The removal of  $Pb^{+2}$  ions on all adsorbent obeys a pseudo-second-order model. The adsorption thermodynamic showed a negative value of free energy ( $\Delta G^\circ$ ) and enthalpy ( $\Delta H^\circ$ ) which indicates that the adsorption of lead (II) on that composites NMO / (4M, 6M, 8M) AC is a spontaneous process and exothermic in nature of the reaction. Finally, a novel prepared composite NMO / (4M,6M,8M) AC were proposed for adsorption of lead (II) from liquid waste taking advantage of its high removal efficiency, low cost, excellent stability and simple preparation.

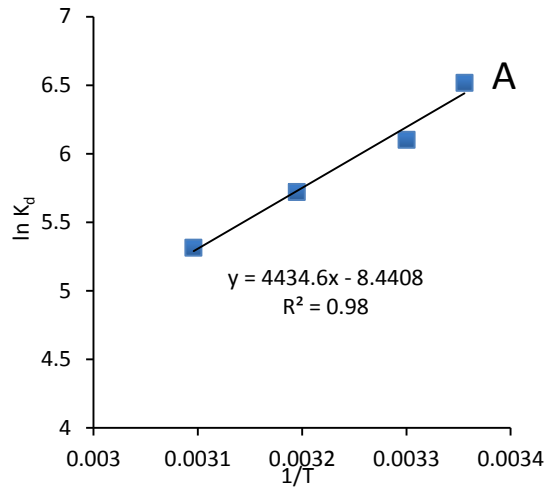


Figure 10(A). Van't Hoff plot for adsorption lead (Pb) ions on sample NMO/4M AC

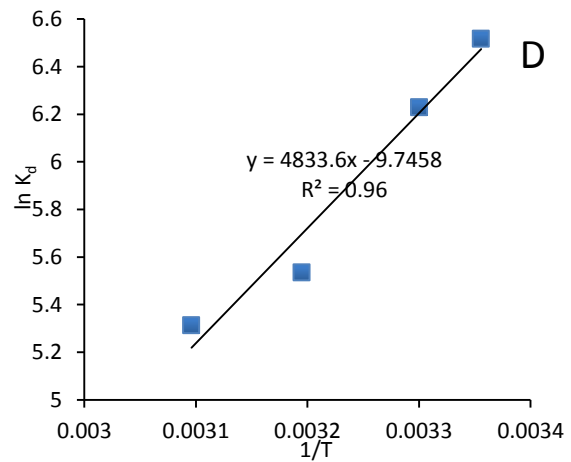


Figure 10(D). Van't Hoff plot for adsorption lead (Pb) ions on sample NMO

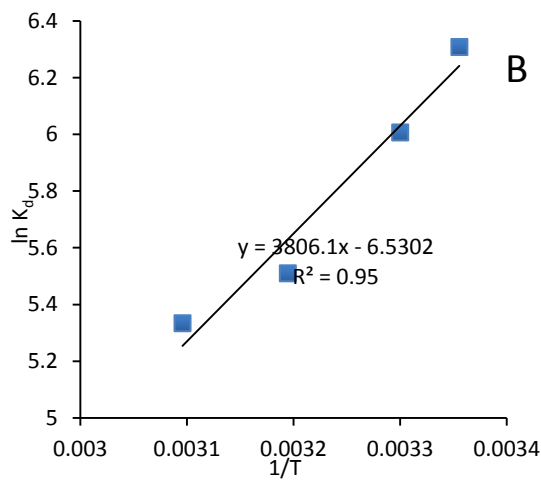


Figure 10(B). Van't Hoff plot for adsorption lead (Pb) ions on sample NMO/6M AC

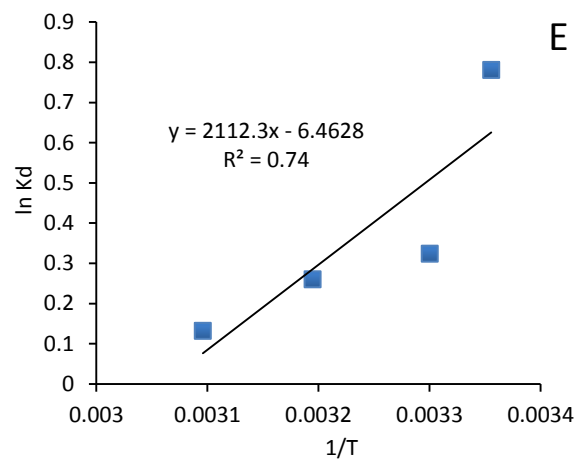


Figure 10(E). Van't Hoff plot for adsorption lead (Pb) ions on sample AC

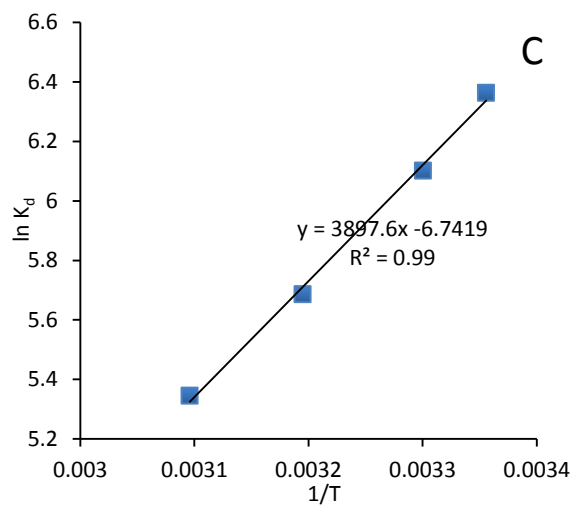


Figure 10(C). Van't Hoff plot for adsorption lead (Pb) ions on sample NMO/8M AC

## Reference

1. Mousa, S. M., Ammar, N. S., and Ibrahim, H. A. (2016): "Removal of lead ions using hydroxyapatite nano-material prepared from phosphogypsum waste". *Journal of Saudi Chemical Society*, 20(3), 357-365.
2. Pandey, P. K., Sharma, S. K., and Sambhi, S. S. (2015): "Removal of lead (II) from waste water on zeolite-NaX". *Journal of Environmental Chemical Engineering*, 3(4), 2604-2610.
3. Fu, F., and Wang, Q. (2011): "Removal of heavy metal ions from wastewaters: a review". *Journal of environmental management*, 92(3), 407-418.
4. Wang, L. K., Vaccari, D. A., Li, Y., and Shamma, N. K. (2005): "Chemical precipitation". In *Physicochemical treatment processes* (pp. 141-197). Humana Press.

5. Walsh, F., C., and Reade, G., W. (1994): "Electrochemical techniques for the treatment of dilute metal-ion solutions". *Studies in environmental science* 59: 3-44.
6. Bodalo-Santoyo, A., Gómez-Carrasco, J., L., Gomez-Gomez, E., Maximo-Martin, F., and Hidalgo-Montesinos, A. M. (2003): "Application of reverse osmosis to reduce pollutants present in industrial wastewater". *Desalination*, 155(2), 101-108.
7. Ersahin, M., E., Ozgun, H., Dereli, R., K., Ozturk, I., Roest, K., and van Lier, J., B. (2012). "A review on dynamic membrane filtration: materials, applications and future perspectives". *Bioresource technology*, 122, 196-206.
8. Zhang, P., Hahn, H., H., and Hoffmann, E. (2003): "Different behavior of iron (III) and aluminum (III) salts to coagulate silica particle suspension". *Acta hydrochimica et hydrobiologica*, 31(2), 145-151.
9. Xing, Y., Chen, X., and Wang, D. (2007): "Electrically regenerated ion exchange for removal and recovery of Cr (VI) from wastewater". *Environmental science & technology*, 41(4), 1439-1443.
10. Srivastava, V., Weng, C. H., Singh, V. K., and Sharma, Y. C. (2011): "Adsorption of nickel ions from aqueous solutions by nano alumina: kinetic, mass transfer, and equilibrium studies". *Journal of Chemical & Engineering Data*, 56(4), 1414-1422.
11. Batley, G. E., and Farrar, Y. J. (1978): "Irradiation techniques for the release of bound heavy metals in natural waters and blood". *Analytica Chimica Acta*, 99(2), 283-292.
12. Rykowska, I., Wasiak, W., and Byra, J. (2008): "Extraction of copper ions using silica gel with chemically modified surface". *Chemical Papers*, 62(3), 255-259.
13. Babu, B. V., and Gupta, S. (2004): "Modeling and simulation for dynamics of packed bed adsorption". In *Proceedings of International Symposium & 57th Annual Session of IChE in association with AIChE (CHEMCON-2004)*, Mumbai
14. Cao, J., Mao, Q., Shi, L., and Qian, Y. (2011): "Fabrication of  $\gamma$ -MnO<sub>2</sub>/ $\alpha$ -MnO<sub>2</sub> hollow core/shell structures and their application to water treatment". *Journal of materials chemistry*, 21(40), 16210-16215.
15. Robinson, D. M., Go, Y. B., Mui, M., Gardner, G., Zhang, Z., Mastrogiovanni, D., and Dismukes, G. C. (2013): "Photochemical water oxidation by crystalline polymorphs of manganese oxides: structural requirements for catalysis". *Journal of the American chemical Society*, 135(9), 3494-3501.
16. Débart, A., Paterson, A. J., Bao, J., and Bruce, P. G. (2008): " $\alpha$ -MnO<sub>2</sub> Nanowires: A Catalyst for the O<sub>2</sub> Electrode in Rechargeable Lithium Batteries". *Angewandte Chemie International Edition*, 47(24), 4521-4524.
17. Yan, D., Cheng, S., Zhuo, R. F., Chen, J. T., Feng, J. J., Feng, H. T., and Yan, P. X. (2009): "Nanoparticles and 3D sponge-like porous networks of manganese oxides and their microwave absorption properties". *Nanotechnology*, 20(10), 105706.
18. Lang, X., Hirata, A., Fujita, T., and Chen, M. (2011): "Nanoporous metal/oxide hybrid electrodes for electrochemical supercapacitors". *Nature nanotechnology*, 6(4), 232.
19. Li, L., Nan, C., Lu, J., Peng, Q., and Li, Y. (2012): " $\alpha$ -MnO<sub>2</sub> nanotubes: high surface area and enhanced lithium battery properties". *Chemical Communications*, 48(55), 6945-6947.
20. Zhong, K., Zhang, B., Luo, S., Wen, W., Li, H., Huang, X., and Chen, L. (2011): "Investigation on porous MnO microsphere anode for lithium ion batteries". *Journal of Power Sources*, 196(16), 6802-6808.
21. Wu, M. S., Chiang, P. C. J., Lee, J. T., and Lin, J. C. (2005): "Synthesis of manganese oxide electrodes with interconnected nanowire structure as an anode material for rechargeable lithium ion batteries". *The Journal of Physical Chemistry B*, 109(49), 23279-23284.
22. García-García, A., Gregório, A., Franco, C., Pinto, F., Boavida, D., and Gulyurtlu, I. (2003): "Unconverted chars obtained during biomass gasification on a pilot-scale gasifier as a source of activated carbon production". *Bioresource Technology*, 88(1), 27-32.
23. Rivera-Utrilla, J., Sánchez-Polo, M., Gómez-Serrano, V., Álvarez, P. M., Alvim-Ferraz, M. C. M., and Dias, J. M. (2011): "Activated carbon modifications to enhance its water treatment applications. An overview". *Journal of Hazardous Materials*, 187(1-3), 1-23.
24. Rivera-Utrilla, J., and Sánchez-Polo, M. (2003): "Adsorption of Cr(III) on ozonised activated carbon. Importance of C $\pi$ -cation interactions". *Water Research*, 37(14), 3335-3340.
25. Yin, C., Aroua, M., and Daud, W. (2007): "Review of modifications of activated carbon for enhancing contaminant uptakes from aqueous solutions". *Separation and Purification Technology*, 52(3), 403-415.
26. Strelko, V., and Malik, D. J. (2002): "Characterization and Metal Sorptive

- Properties of Oxidized Active Carbon". *Journal of Colloid and Interface Science*, 250(1), 213–220.
27. Pradhan, B. K., and Sandle, N. K. (1999): "Effect of different oxidizing agent treatments on the surface properties of activated carbons". *Carbon*, 37(8), 1323-1332.
  28. Daud, W. M. A. W., and Houshamnd, A. H. (2010): "Textural characteristics, surface chemistry and oxidation of activated carbon". *Journal of Natural Gas Chemistry*, 19(3), 267-279.
  29. Chen, J. P., and Wu, S. (2004): "Acid/base-treated activated carbons: characterization of functional groups and metal adsorptive properties". *Langmuir*, 20(6), 2233-2242.
  30. Abdellah, W. M., El-Ahwany, H. I., and El-Sheikh, R. (2020) "Removal of Technetium (99Tc) from aqueous waste by manganese oxide nanoparticles loaded into activated". *Open Journal of Applied Sciences, JASMI Vol10, No 1*.
  31. Abdullah, N., Yusof, N., Ismail, A. F., Ermala, F., Othman, C., and Jaafar, J. (2018): "Effects of manganese (VI) oxide on polyacrylonitrile-based activated carbon nanofibers (ACNFs) and its preliminary study for adsorption of lead (II) ions". *Emergent Materials*, 1(1-2), 89-94.
  32. Holm, E., Gäfvert, T., Lindahl, P., and Roos, P. (2000): "In situ sorption of technetium using activated carbon". *Applied Radiation and Isotopes*, 53(1-2), 153-157.
  33. Al Abdullah, J., Al Lafi, A. G., Amin, Y., and Alnana, T. (2016): "Adsorption of cesium, cobalt, and lead onto a synthetic nano manganese oxide: behavior and mechanism". *Water, Air, & Soil Pollution*, 227(7), 241.
  34. Telkapalliwar, N., and Shivankar, V. (2016): "Adsorption of Pb (II) from aqueous solution onto microwave assisted activated carbon prepared from orange peel". *Int J Appl InnovEngManag*, 5, 76-82.
  35. Chen, A. H., Yang, C. Y., Chen, C. Y., Chen, C. Y., and Chen, C. W. (2009): "The chemically crosslinked metal-complexed chitosans for comparative adsorptions of Cu (II) ,Zn (II) ,Ni (II) and Pb (II) ions in aqueous medium". *Journal of Hazardous Materials*, 163(2-3), 1068-1075.
  36. Ali, I. (2012): "New generation adsorbents for water treatment". *Chemical reviews*, 112(10), 5073-5091.
  37. Tan, I. A. W., Ahmad, A. L., and Hameed, B. H. (2009): "Adsorption isotherms, kinetics, thermodynamics and desorption studies of 2, 4, 6-trichlorophenol on oil palm empty fruit bunch-based activated carbon". *Journal of Hazardous Materials*, 164(2-3), 473-482.
  38. Shen, W., Chen, S., Shi, S., Li, X., Zhang, X., Hu, W., and Wang, H. (2009): "Adsorption of Cu (II) and Pb (II) onto diethylenetriamine-bacterial cellulose". *Carbohydrate Polymers*, 75(1), 110-114.
  39. Ho, Y. S., Chiu, W. T., and Wang, C. C. (2005): "Regression analysis for the sorption isotherms of basic dyes on sugarcane dust". *Bioresource technology*, 96(11), 1285-1291.
  40. Weber, T. W., and Chakravorti, R. K. (1974): "Pore and solid diffusion models for fixed-bed adsorbents". *AIChE Journal*, 20(2), 228-238.
  41. Goel, J., Kadirvelu, K., Rajagopal, C., and Kumar Garg, V. (2005): "Removal of lead (II) by adsorption using treated granular activated carbon: Batch and column studies". *Journal of Hazardous Materials*, 125(1-3), 211–220.
  42. Acharya, J., Sahu, J. N., Mohanty, C. R., and Meikap, B. C. (2009): "Removal of lead (II) from wastewater by activated carbon developed from Tamarind wood by zinc chloride activation". *Chemical Engineering Journal*, 149(1-3), 249-262.
  43. Mellah, A., Chegrouche, S., and Barkat, M. (2006): "The removal of uranium (VI) from aqueous solutions onto activated carbon: kinetic and thermodynamic investigations". *Journal of colloid and interface science*, 296(2), 434-441.
  44. Chanda, M., and Rempel, G. L. (1992): "Uranium sorption behavior of a macroporous, quaternized poly (4-vinylpyridine) resin in sulfuric acid medium". *Reactive polymers*, 18(2), 141-154.
  45. Ho, Y. S., and McKay, G. (1998): "A comparison of chemisorption kinetic models applied to pollutant removal on various sorbents". *Process safety and environmental protection*, 76(4), 332-340.
  46. Liu, Z., Zhong, X., Wang, Y., Ding, Z., Wang, C., Wang, G., and Liao, S. (2018): "An efficient adsorption of manganese oxides/activated carbon composite for lead (II) ions from aqueous solution". *Arabian Journal for Science and Engineering*, 43(5), 2155-2165.
  47. Acharya, J., Sahu, J. N., Sahoo, B. K., Mohanty, C. R., and Meikap, B. C. (2009): "Removal of chromium (VI) from wastewater by activated carbon developed from Tamarind wood activated with zinc chloride". *Chemical Engineering Journal*, 150(1), 25-39.
  48. El-Wakeel, S. T., El-Tawil, R. S., Abuzeid, H. A. M., Abdel-Ghany, A. E., and Hashem, A. M. (2017): "Synthesis and structural properties of MnO<sub>2</sub> as adsorbent for the removal of lead (Pb<sup>2+</sup>) from aqueous solution". *Journal of the*

- 
- Taiwan Institute of Chemical Engineers, 72, 95–103.
49. Qiu, W., Yang, D., Xu, J., Hong, B., Jin, H., Jin, D., and Wang, X. (2016): "Efficient removal of Cr(VI) by magnetically separable CoFe<sub>2</sub>O<sub>4</sub>/activated carbon composite". *Journal of Alloys and Compounds*, 678, 179–184.